Synthesis, Molecular and Crystal Structure of Tetraruthenium Butterfly Arene Clusters†

Dario Braga,*[a] **Fabrizia Grepioni,**[a] **Janice J. Byrne,**[a] **Caroline M. Martin,**[b] **Brian F. G. Johnson***[b] **and Alexander J. Blake**[b]
[a] *Dipartimento di Chimica G. Ciamician, Università di Bologna, Via Selmi 2, 40126 Bologna, Italy*
[b] *Department of Chemistry, The University of Edinburgh, West Mains Road, Edinburgh EH9 3JJ, UK*

A series of Ru_4 butterfly cluster complexes have been synthesized and investigated by spectroscopic and diffraction methods. The solid-state structure of $[Ru_4(CO)_{12}(\mu_4\text{-}\eta^2:\eta^2\text{-}C_6H_8)]$ **1** and of the two isomers of $[Ru_4(CO)_9(\mu_4\text{-}\eta^2:\eta^2\text{-}C_6H_8)(\eta^6\text{-}C_6H_6)]$ with the benzene ring located on the butterfly hinge (**2**) or on the wingtip (**3**), have been characterized. The three complexes are monoclinic, **1**: space group $P2_1/c$, $a = 9.779(8)$, $b = 22.163(14)$, $c = 10.069(6)$ Å, $\beta = 90.23(9)°$, $Z = 4$; **2**: space group Cc, $a = 10.010(3)$, $b = 15.532(4)$, $c = 15.384(4)$ Å, $\beta = 93.50(2)°$, $Z = 4$; **3**: space group $P2_1/c$, $a = 16.655(3)$, $b = 15.709(3)$, $c = 17.831(4)$ Å, $\beta = 91.44(3)°$, $Z = 8$. The molecular structures of the complexes have been investigated in relation with the respective crystal structure and, in the case of **2**, compared with the polymorphic modification described previously.

We have been actively concerned with an investigation into the chemistry of organo-cluster compounds and in particular with the dehydrogenation reactions that certain cyclic olefins undergo to produce arene and cyclohexyne derivatives. The factors which control the activation of C–H bonds by clusters are difficult to define but are clearly of considerable significance. Recently, as part of these studies we have reported the synthesis and full chemical and structural characterization of a number of isomeric cluster systems which differ *either* in the bonding mode adopted by the arene (η^6-terminal or μ_3-face bridging) or in the site of attachment (*e.g.* the axial or basal metal atom in the Ru_5C square-pyramidal unit).[1] These various isomeric types have been observed mainly for the families of compounds obtained from the Ru_5 and Ru_6 cluster units.[2] Extended-Hückel calculations[3] have contributed to the rationalization of the relative stabilities of the various isomer forms showing, for example, that in the case of the *bis*-benzene species, *cis*-$[Ru_6C(CO)_{11}(\eta^6\text{-}C_6H_6)_2]$, $[Ru_6C(CO)_{11}(\eta^6\text{-}C_6H_6)(\mu_3\text{-}\eta^2:\eta^2:\eta^2\text{-}C_6H_6)]$ and *trans*-$[Ru_6C(CO)_{11}(\eta^6\text{-}C_6H_6)_2]$, the most stable isomer is that carrying the two benzene ligands in *cis*-positions on two adjacent Ru atoms and that the apical–facial isomer is formed first mainly for kinetic reasons. This behaviour is in accordance with the interconversion reactions observed in solution. It has also been possible to demonstrate that the crystal-packing forces stabilize the less favourable isomers because the energy difference is small and comparable to those of intermolecular interactions.[3] The basic packing motifs observed in these crystalline materials are: (*i*) arene–arene interaction of the graphitic type between the arene ligands belonging to neighbouring molecules; (*ii*) carbonyl–carbonyl interactions based on the interlocking of tri- or tetra-carbonyl units as commonly observed in carbonyl cluster systems; and (*iii*) carbonyl–arene interactions most often based on intricate networks of C–H ··· O hydrogen bonds.[4] This latter type of interaction has been observed in a number of neutral organometallic systems.[3,5] Hydrogen bonding of the O–H ··· O and C–H ··· O type in organometallic systems has been recently subjected to systematic investigations.[6]

In this study we focus our interest on the relationship between *molecular* and *crystal* structures of the tetranuclear clusters $[Ru_4(CO)_{12}(\mu_4\text{-}\eta^2:\eta^2\text{-}C_6H_8)]$ **1** and of the two isomeric forms of the benzene derivative $[Ru_4(CO)_9(\mu_4\text{-}\eta^2:\eta^2\text{-}C_6H_8)(\eta^6\text{-}C_6H_6)]$ which differ in the location of the benzene ligand [butterfly hinge (**2**), wingtip (**3**)]. It is of some interest also to compare the crystal structure of **2** with that of a polymorphic modification reported previously.[7]

Results and Discussion

Synthesis and Chemical Characterization.—The thermolysis of $[Ru_3(CO)_{12}]$ in octane containing cyclohexa-1,3-diene affords a range of products, in varying yields, four of which have been isolated and identified. The two major products obtained from the reaction are the tetranuclear cluster $[Ru_4(CO)_{12}(\mu_4\text{-}\eta^2:\eta^2\text{-}C_6H_8)]$ **1** and the known hexanuclear carbido cluster $[Ru_6C(CO)_{14}(\eta^6\text{-}C_6H_6)]$ **4**; however, two isomeric products with formula $[Ru_4(CO)_9(\mu_4\text{-}\eta^2:\eta^2\text{-}C_6H_8)(\eta^6\text{-}C_6H_6)]$ (**2** and **3**) have also been isolated; the 'hinge' isomer **2** being produced in greater yield than the 'wingtip' isomer **3**. Spectroscopic properties for **1**–**3** are reported in Table 1. In a series of separate experiments we have further established that **2** is the major product obtained from the thermolysis of **1** in octane containing cyclohexa-1,3-diene, yet the reaction of **1** with Me_3NO in the presence of cyclohexa-1,3-diene at room temperature affords mainly **3**. Furthermore, on heating in octane, compound **3** is quantitatively converted into **2** which then slowly (and not quantitatively) converts back into **3** at room temperature. This series of reactions are summarized in Scheme 1.

The hexanuclear carbido cluster $[Ru_6C(CO)_{14}(\eta^6\text{-}C_6H_6)]$ **4** has been previously observed on several occasions and its molecular structure determined by single-crystal X-ray analysis.[2] Compounds **1**–**3** were initially characterized on the basis of the customary analytical and spectroscopic techniques, and their molecular structures determined by X-ray diffraction methods on crystals grown from toluene solutions at −25 °C (**1** and **2**) and from the slow evaporation of a dichloromethane–hexane solution (**3**).

The infrared spectrum (ν_{CO}) of **1** is very similar, in both symmetry and wavenumber, to those observed for the related alkyne compounds $[Ru_4(CO)_{12}(\mu_4\text{-}\eta^2:\eta^2\text{-}C_2Ph_2)]$[8] and $[Ru_4(CO)_{12}(\mu_4\text{-}\eta^2:\eta^2\text{-}C_2Me_2)]$,[9] with peaks between 2064 and 1970

---

† *Supplementary data available:* see Instructions for Authors, *J. Chem. Soc., Dalton Trans.*, 1995, Issue 1, pp. xxv–xxx.

Non-SI unit employed: cal ≈ 4.184 J.

Table 1 Spectroscopic data for compounds 1–3

Compound	IR(ν_{CO}/cm^{-1}, CH_2Cl_2)	M^{+}*	^{1}H NMR (δ, $CDCl_3$)	Microanalysis* (%) C	Microanalysis* (%) H
1 [$Ru_4(CO)_{12}(\mu_4$-$C_6H_8)$]	2091w, 2064s, 2034vs, 2009m, 1968w (sh)	821 (821)	3.35 (m, 4 H), 1.82 (m, 4 H)	26.30 (26.35)	0.90 (1.00)
2 [$Ru_4(CO)_9(\mu_4$-$C_6H_8)(\eta^6$-$C_6H_6)$] 'Hinge' isomer	2060m, 2035vs, 2010s, 1981s, 1969m (sh), 1924w	815 (815)	5.52 (s, 6 H), 3.27 (m, 4 H), 1.82 (m, 4 H)	31.00 (30.95)	1.45 (1.70)
3 [$Ru_4(CO)_9(\mu_4$-$C_6H_8)(\eta^6$-$C_6H_6)$] 'Wingtip' isomer	2065s, 2022s, 2009vs, 1993w (sh), 1958m	816 (815)	5.67 (s 6 H), 3.37 (m, 4 H), 1.80 (m, 4 H)	31.05 (30.95)	1.50 (1.70)

* Calculated values in parentheses.

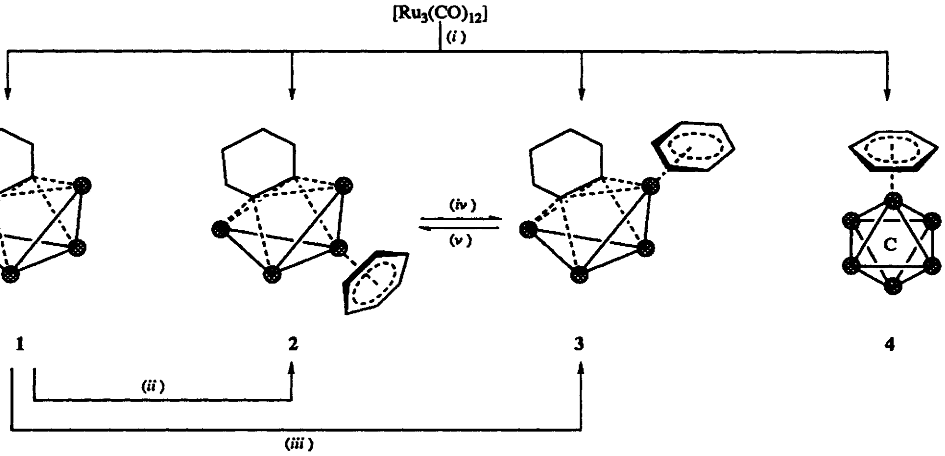

Scheme 1 The reaction of [$Ru_3(CO)_{12}$] with cyclohexa-1,3-diene, and the interconversion of the resulting products. (*i*) Heat, octane–1,3-C_6H_8; (*ii*) heat, octane–1,3-C_6H_8; (*iii*) Me_3NO (3.2 equivalents), CH_2Cl_2–1,3-C_6H_8, −78 °C; (*iv*) CH_2Cl_2, room temperature; (*v*) heat, octane

cm^{-1} that are typical of terminal carbonyls. The mass spectrum of 1 exhibits a parent peak at *m*/*z* 821 (calc. 821) followed by the loss of twelve carbonyl groups in succession. The ^{1}H NMR spectrum contains two multiplet resonances at δ 3.35 and 1.82 with equal relative intensities, which can be assigned to the eight aliphatic ring protons of the cyclohexyne moiety. As anticipated, X-ray diffraction analyses show that the compound consists of a Ru_4 butterfly framework with a cyclohexyne ligand, produced from the isomerization of cyclohexadiene, trapped between the two butterfly wings and three terminal carbonyl ligands on each of the four ruthenium atoms (see below). The infrared spectra of the two isomers 2 and 3 also show peaks in the terminal carbonyl region only (2060–1924 and 2065–1958 cm^{-1} for 2 and 3, respectively) with that of 2 being almost identical to that of the polymorph 2a reported by Aime *et al.*[7] The mass spectra of 2 and 3 exhibit parent ion peaks at *m*/*z* 815 and 816 (calc. 815) respectively, followed by the sequential loss of several carbonyl groups.

The ^{1}H NMR spectra are also very similar with both complexes showing three resonances; a singlet and two multiplets with relative intensities 3:2:2, corresponding to the six protons of the benzene ring and the eight protons of the cyclohexyne moiety [2 δ 5.52 (s, 6 H), 3.27 (m, 4 H), 1.82 (m, 4 H); 3 δ 5.67 (s, 6 H), 3.37 (m, 4 H), 1.80 (m, 4 H)]. The singlet resonances at δ 5.52 and 5.67 for 2 and 3 respectively are consistent with η^6-terminally co-ordinated benzene ligands. X-Ray diffraction analyses show that the isomers 2 and 3 contain the same general features as 1; in 2, however, three carbonyls on a 'hinge' ruthenium atom have been replaced by the benzene moiety (which is produced by the dehydrogenation of cyclohexadiene), whereas in 3 the benzene adopts the wingtip position.

Mechanistic Proposals.—The wingtip isomer 3 is formed preferentially from the reaction of [$Ru_4(CO)_{12}(\mu_4$-η^2:η^2-$C_6H_8)$] 1 with Me_3NO in the presence of C_6H_8. On heating 1 with C_6H_8 the alternative hinge isomer 2 is produced, and 3 undergoes conversion to 2 on heating. On standing under ambient conditions, however, 2 slowly reverts back into 3. We have previously noted similar behaviour for the related Ru_5C system,[10] and we believe that two distinctly different isomerization mechanisms operate. One involves the slippage of the benzene moiety over the cluster framework (hinge-to-wingtip) possibly *via* the intermediacy of an edge-bridged arene molecule (see Scheme 2). This is a low energy process and therefore occurs at ambient temperature. The second occurs *via* a polyhedral rearrangement of the *quasi*-octahedral Ru_4C_2 central cluster core *via* a trigonal-prismatic complementary geometry (wingtip-to-hinge, see Scheme 3). In an alternative view of this process the Ru_4 butterfly arrangement may be considered to form a square plane (cleavage of one Ru–Ru bond), whilst the organo-bridge rotates about the four Ru atoms. Intuitively one would view this as a relatively high energy process, taking place upon heating. A combination of these two mechanisms produces the cyclic process illustrated in Scheme 4.

Also of interest is the reaction of Me_3NO. Clearly attack appears to occur preferentially at the wingtip $Ru(CO)_3$ unit, indicating an enhanced nucleophilicity of the bonded CO groups at this site.

Molecular Structures of 1–3 *in the Solid State.*—The molecular structures of [$Ru_4(CO)_{12}(\mu_4$-η^2:η^2-$C_6H_8)$] 1, [$Ru_4(CO)_9(\mu_4$-η^2:η^2-$C_6H_8)(\eta^6$-$C_6H_6)$] hinge isomer 2 and [$Ru_4(CO)_9(\mu_4$-η^2:η^2-$C_6H_8)(\eta^6$-$C_6H_6)$] wingtip isomer 3 are shown in Figs. 1, 2 and 3, respectively, together with the labelling schemes. Relevant structural parameters are compared in Table 2. Due to the presence of two independent molecules in the asymmetric unit of 3, two sets of parameters are reported (3a and 3b). The three clusters have the same metal skeleton. They are characterized by a Ru_4 butterfly cluster with a cyclohexyne ligand trapped between the two wingtips. This ligand donates a total of six electrons to the cluster framework *via* two π interactions with the hinge atoms and two σ interactions with

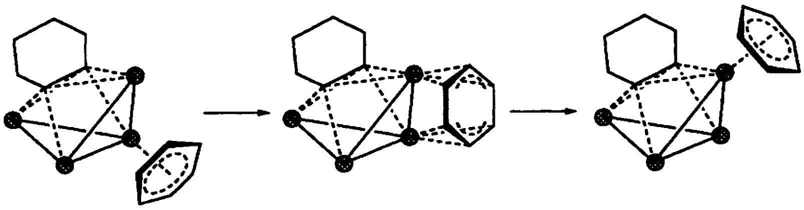

2 3

Scheme 2 A possible mechanism for the conversion of **2** into **3** at room temperature

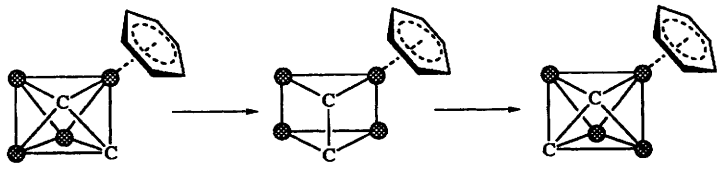

'Wingtip isomer **3** 'Hinge' isomer **2**

Scheme 3 A possible mechanism for the conversion of **3** into **2** at 125 °C

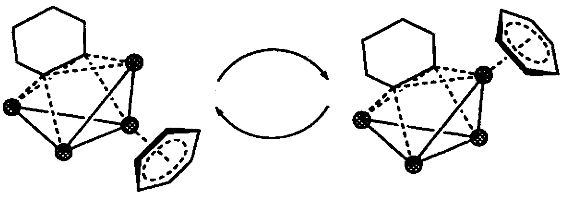

2 3

Scheme 4 The observed cyclic process observed from a combination of Schemes 2 and 3

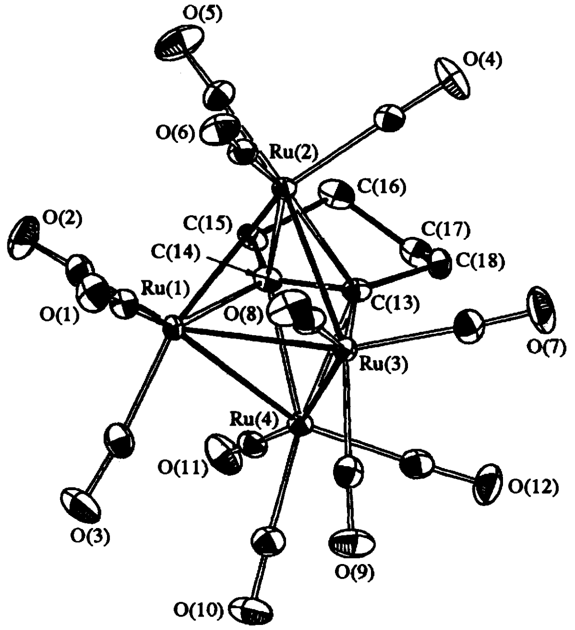

Fig. 1 The molecular structure of $[Ru_4(CO)_{12}(\mu_4\text{-}\eta^2:\eta^2\text{-}C_6H_8)]$ **1** in the solid state showing the anisotropic thermal parameters and the atomic labelling scheme

the wingtip atoms. This gives a total of fourteen electrons which correspond to a *closo*-octahedral arrangement ($N = 7$). This electron transfer from the acetylenic bond gives rise to a lengthening of the C–C bond [C(13)–C(14) is 1.455(7) in **1**, 1.43(1) in **2** and 1.46(2) Å in **3** (this latter value is averaged over **3a** and **3b**)]. The conformation of the ligand is that of a 'half chair' due to the bonding and steric requirements of the metal cluster.

In the case of **1** each metal is co-ordinated by three terminal carbonyl groups. The formal loss of three carbonyl groups from

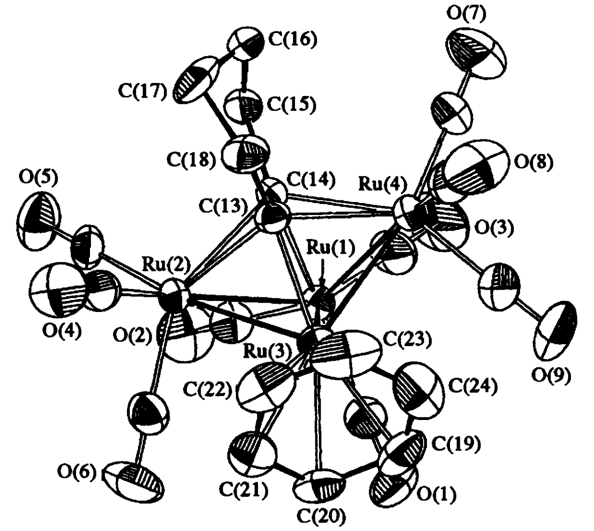

Fig. 2 The molecular structure of $[Ru_4(CO)_9(\mu_4\text{-}\eta^2:\eta^2\text{-}C_6H_8)(\eta^6\text{-}C_6H_6)]$ hinge isomer **2** in the solid state showing the anisotropic thermal parameters and the atomic labelling scheme

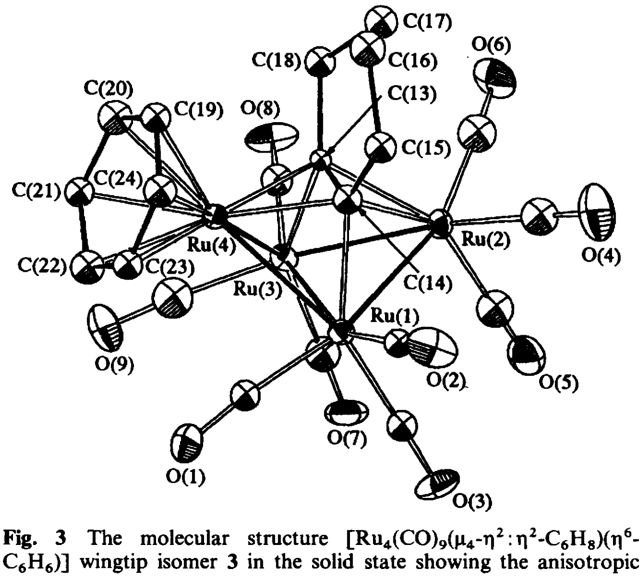

Fig. 3 The molecular structure $[Ru_4(CO)_9(\mu_4\text{-}\eta^2:\eta^2\text{-}C_6H_8)(\eta^6\text{-}C_6H_6)]$ wingtip isomer **3** in the solid state showing the anisotropic thermal parameters and the atomic labelling scheme

Table 2 Selected bond lengths (Å) and angles (°) for **1**–**3***

	1	**2**	**3a**	**3b**
Ru(1)–Ru(2)	2.743(2)	2.7057(8)	2.733(2)	2.731(2)
Ru(1)–Ru(3)	2.849(3)	2.8105(8)	2.812(2)	2.812(2)
Ru(1)–Ru(3)	2.725(2)	2.6940(8)	2.728(2)	2.708(2)
Ru(2)–Ru(3)	2.727(2)	2.6476(7)	2.722(2)	2.729(2)
Ru(3)–Ru(4)	2.721(2)	2.6579(5)	2.707(2)	2.739(2)
Ru(1)–C(14)	2.123(5)	2.170(5)	2.11(2)	2.18(2)
Ru(3)–C(13)	2.146(4)	2.073(5)	2.15(2)	2.16(2)
Ru(2)–C(13)	2.243(5)	2.223(5)	2.21(2)	2.29(2)
Ru(2)–C(14)	2.244(4)	2.245(5)	2.26(2)	2.25(2)
Ru(4)–C(13)	2.234(5)	2.251(5)	2.18(2)	2.14(2)
Ru(4)–C(14)	2.246(5)	2.272(5)	2.16(2)	2.20(2)
C(13)–C(14)	1.455(7)	1.43(1)	1.45(3)	1.48(3)
C(14)–C(15)	1.534(6)	1.52(1)	1.57(3)	1.52(3)
C(15)–C(16D)		1.49(1)		
C(15)–C(16)	1.525(7)	1.52(1)	1.60(3)	1.53(3)
C(16D)–C(17D)		1.46(2)		
C(16)–C(17)	1.505(7)	1.53(2)	1.56(3)	1.51(3)
C(17)–C(18)	1.543(6)	1.51(1)	1.50(3)	1.56(3)
C(17D)–C(18)		1.51(2)		
C(13)–C(18)	1.521(7)	1.54(1)	1.57(3)	1.53(3)
C(13)–C(14)–C(15)	121.4(4)	122(1)	123(2)	123(2)
C(14)–C(15)–C(16)	112.2(4)	110(1)	113(2)	110(2)
C(14)–C(15)–C(16D)		115(1)		
C(15)–C(16)–C(17)	110.9(4)	110(1)	111(2)	112(2)
C(15)–C(16D)–C(17D)		113(2)		
C(16)–C(17)–C(18)	111.2(4)	109(1)	113(2)	115(2)
C(16D)–C(17D)–C(18)		118(2)		
C(17)–C(18)–C(13)	110.4(4)	112(1)	112(2)	110(2)
C(18)–C(13)–C(14)	121.5(4)	121(1)	120(2)	122(2)
Ru–C(19)		2.207(7)	2.21(2)	2.19(2)
Ru–C(20)		2.239(6)	2.23(2)	2.19(2)
Ru–C(21)		2.260(7)	2.23(2)	2.22(2)
Ru–C(22)		2.208(6)	2.19(2)	2.19(2)
Ru–C(23)		2.184(7)	2.19(2)	2.18(2)
Ru–C(24)		2.225(7)	2.23(2)	2.19(2)
Ru–(CO)(mean)	1.912(5)	1.897(7)	1.92(2)	1.92(2)
C–O(CO)(mean)	1.136(6)	1.136(9)	1.14(3)	1.12(3)

* D = Disordered atom.

a hinge atom and replacement by an η^6-benzene results in the structure of **2**, while the formal replacement of three carbonyls from a wingtip metal atom by an η^6-benzene ligand leads to the structure of **3**.

The hinge bond in **1** is significantly longer than the other bonds [2.849(3) Å *vs.* 2.721(2)–2.743(2) Å]. Each Ru atom bears three terminal carbonyl groups [average Ru–C(CO) bond distance 1.912(5) Å]. The two Ru–C σ bonds formed by C(13) and C(14) with the hinge atoms of the cluster [2.146(4) and 2.123(5) Å respectively] are shorter than the two π bonds with the atoms of the wingtips [Ru(2)–C(13) 2.243(5), Ru(4)–C(13) 2.234(5), Ru(2)–C(14) 2.244(4) and Ru(4)–C(14) 2.246(5) Å].

The same basic cluster structure of **1** is retained on replacement of the three terminal CO atoms on Ru(3) by a benzene ligand. The C_6H_8 unit is disordered showing two orientations of the outer part of the ring. These two different possibilities for ring orientation are equivalent by idealized molecular symmetry and are equally occupied in the solid state. Since ring-flip in the solid state is a well established phenomenon, the possibility that the disorder in **2** arises from a dynamic process had to be considered.[11] The flipping of the C_6H_8 ring from one conformation to the other was simulated *via* a rotation of the $H_2C(16)$–$C(17)H_2$ unit about the axis passing through the midpoint of the C–C bond and the midpoint of the C(13)–C(14) bond. The intermolecular atom–atom potential energy was recalculated at 10° rotational steps for a full 360° rotation. Similar procedures have been applied previously with success to the rationalization of several dynamic processes occurring in the solid state.[11] In order to avoid any problem caused by the positions of the hydrogens in this model, the CH_2 groups were replaced by larger van der Waals spheres and attributed the potential parameters of Cl atoms.[12] Although the model is admittedly crude, it allows a comparison between the two conformations. The barrier to interconversion was found to be very low (*ca.* 0.8 kcal mol^{-1}) which allows us to state with some degree of confidence that the disorder in the crystal structure of **2** is very likely to be dynamic in origin.

A marked difference between **1** and **2** is seen in both the average metal–metal bond distance and the average metal–carbon bond distance. The average Ru–Ru bond is shortened with respect to **1** [2.7031(8) *vs.* 2.753(2) Å]. There are three terminal carbonyl ligands on Ru(1), Ru(2) and Ru(4). The average Ru–C(CO) distance is also comparably short in **2** [1.897(7) *vs.* 1.912(5) Å in **1**]. As in the case of structure **1** the hinge Ru–Ru bond is longer [2.8105(8) Å] than the other Ru–Ru distances [ranging from 2.6476(7) to 2.7057(8) Å].

Previous to our molecular and crystal structure determination for this compound another structure (**2a**) for the same compound had been reported by Aime *et al.*[7] In terms of molecular geometry, this previous structure is quite similar to ours with an average Ru–Ru bond length [2.704(3) Å] and Ru–C(CO) bond length [1.88(1) Å] comparable with those observed for the structure of **2**. However the C_6H_8 ligand does not show disorder.

The structure of **3** can be obtained from that of compound **1** by replacement of the three terminal CO atoms on the wingtip atom Ru(4) by a benzene ring. We see the same basic Ru cluster structure. The asymmetric unit of the crystal cell contains, however, two independent molecules which differ essentially by a slight difference in the orientation of the 'half chair' of the C_6H_8 ligand. The shortening of the bond lengths seen on going from **1** to **2** does not arise on going from **1** to **3**. Again, as in the case of the other structures, the hinge bond is longer [2.812(2) Å in both molecules] than the other Ru–Ru distances [ranging from 2.707(2) to 2.739(2) Å over the two molecules].

Discussion of the Crystal Structures of **1**–**3**.—The crystal structures of species **1**, **2** (both forms) and **3** have been investigated by means of approximate packing potential energy calculations and molecular graphics. The 'decoding' of the molecular organization within the crystal structure is based on an analysis of the immediate neighbourhood of the reference molecule. To this purpose we have applied methods based on atom–atom potential energy calculations[13] which we developed previously to investigate the crystal structures of organometallic materials.[14] The atom–atom pairwise potential energy method allows a rough estimate of the *relative* packing energies for classes of related compounds. Although the method requires some far from trivial approximations in order to be used on complex organometallic systems, it has been found in all previous applications, that it predicts the correct ranking of energy. Hence, we use it here as a shorthand tool to estimate the packing cohesion (p.c.) and the packing potential energy (p.p.e. hereafter) of our complexes. For a detailed discussion the reader is addressed to ref. 14. The volumes of the molecular units were calculated by using literature van der Waals radii for the main group elements and an arbitrary radius of 2.35 Å for the Ru atoms; packing coefficients were estimated as $V_{mol}Z/V_{cell}$. The calculation procedures of V_{mol} and p.c. as well as that of p.p.e., are all implemented within Gavezzotti's OPEC[15] suite of programs. Table 3 lists the results of these calculations. PLATON-90[16] was used to search for possible hydrogen bonds. Prior to its use all C–H bond distances were normalized at 1.08 Å in order for the hydrogens to be located at their nucleus and not at the centre of electron density. The C–H ··· O interactions can also be easily detected on the basis of the donor–acceptor C(CH) ··· O distances (usually in the range 3.00–3.60 Å). Table 3 lists the relevant structural parameters for

Table 3 Results of packing potential energy and volume calculations for $[Ru_4(CO)_{12}(\mu_4\text{-}\eta^2{:}\eta^2\text{-}C_6H_8)]$ **1**, $[Ru_4(CO)_9(\mu_4\text{-}\eta^2{:}\eta^2\text{-}C_6H_8)(\eta^6\text{-}C_6H_6)]$ (hinge isomer **2**, wingtip isomer **3**) and **2a** the polymorphic form of **2**

Complex	**1**	**2**	**2a**	**3**
p.c.*	0.74	0.63	0.64	0.66
p.p.e./kcal mol^{-1}	−75.8	−66.1	−67.7	−70.8
Volume (Å^3)	402.3	379.1	381.5	383.3

* Packing coefficient obtained as p.c. = $V_{mol}Z/V_{cell}$, where V_{mol} and V_{cell} are the molecular and cell volumes respectively.

Table 4 Analysis of potential hydrogen bonds (distances in Å, angles in °)

	C···O	H···O	C–H···O
$[Ru_4(CO)_{12}(C_6H_8)]$ **1**			
C(16)–H(16A)···O(8)	3.35	2.67	120.5
$[Ru_4(CO)_9(C_6H_8)(C_6H_6)]$ **2**			
C(19)–H(19)···O(5)	3.65	2.58	171.1
C(22)–H(22)···O(9)	3.30	2.42	137.1
C(24)–H(24)···O(4)	3.52	2.45	174.2
C(17D)–H(17E)···O(2)	3.34	2.37	147.7
C(21)–H(21)···O(3)	3.64	2.62	156.0
C(16D)–H(16E)···O(1)	3.72	2.67	166.5
$[Ru_4(CO)_9(C_6H_8)(C_6H_6)]$ **2a**			
C(12)–H(121)···O(5)	3.39	2.56	133.1
C(16)–H(161)···O(6)	3.49	2.49	153.0
C(18)–H(181)···O(7)	3.49	2.44	163.3
C(19)–H(191)···O(1)	3.73	2.67	165.6
$[Ru_4(CO)_9(C_6H_8)(C_6H_6)]$ **3**			
C(19)–H(19)···O(32)	3.38	2.56	131.3
C(22)–H(22)···O(5)	3.53	2.47	166.1
C(24)–H(24)···O(8)	3.26	2.49	126.9
C(50)–H(50)···O(3)	3.33	2.54	129.0
C(50)–H(50)···O(7)	3.36	2.49	136.3
C(45)–H(45B)···O(2)	3.40	2.57	133.0
C(47)–C(47A)···O(39)	3.63	2.66	149.2
C(21)–H(21)···O(33)	3.34	2.70	117.4
C(46)–H(46B)···O(34)	3.71	2.70	157.2
C(52)–H(52)···O(37)	3.62	2.67	147.0

these interactions. SCHAKAL92 was used for the graphical representation of the results.[17]

From Table 3 it can be seen that the efficiency of packing, expressed *via* Kitaigorodski's packing coefficient, is much higher in crystalline **1** than in the crystals of the two benzene derivatives (p.c. 0.74 *vs.* 0.63, 0.64 and 0.66). This difference is very large and only seldom encountered in classes of related compounds. It is clearly indicative that the substitution of a flat benzene ligand for the conical tricarbonyl unit causes loss of packing efficiency, very probably by reducing the extent of intermolecular interpenetration. The difference in packing efficiency is also reflected by the values of the p.p.e; the crystal structure of **1** is much more cohesive (−75.8 *vs. ca.* −68 kcal mol^{-1}). Another aspect of interest is related to the polymorphs of the hinge isomers (**2** and **2a**). The disordered structure **2** appears to achieve a slightly less efficient packing than **2a**. The reason for this difference is difficult to grasp. It is well known, however, that most molecules can (at least in principle) crystallize in different polymorphic modifications depending on the crystallization conditions. The loose packing in **2** is most certainly responsible for the presence of two disordered orientations of the diene ligand.

The molecular packing in crystalline **1** is based on the interaction between the C_6H_8 ligands and the CO ligands on a neighbouring molecule. There is only one relatively short CH···OC interaction between atom O(8) and H(16A) (see Table 4). In structure **2** the C–H···O hydrogen bonds involve the carbonyl ligands and the hydrogen atoms of both the C_6H_8 and C_6H_6 ligands. A similar distribution of C–H···O interactions is also present in the previously reported structure **2a** as well as in crystalline **3** (see Table 4).

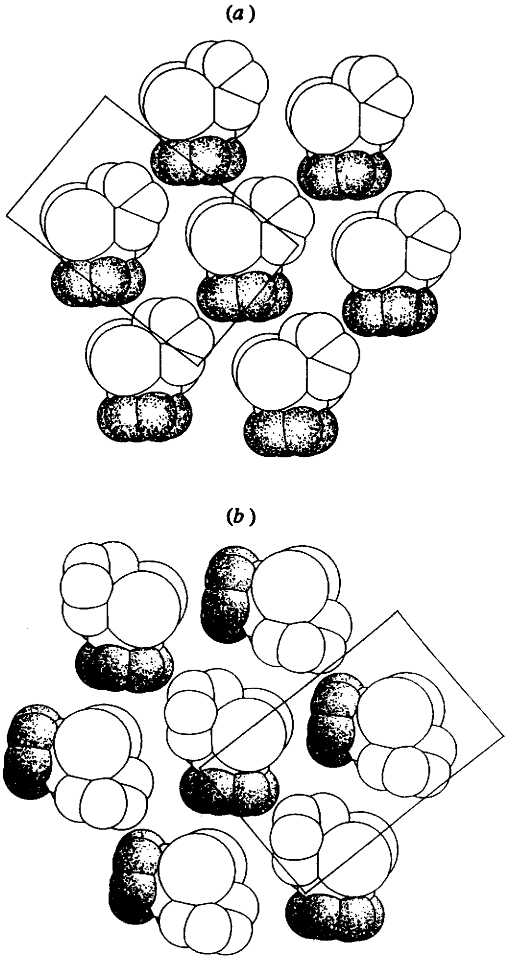

Fig. 4 Comparison of the molecular organization in crystalline **2** (*a*) and **2a** (*b*). Note how, although the molecules are distributed in a very similar way, the benzene ligands are parallel to each other in crystalline **2**, whereas in crystalline **2a** they are at *ca.* 90° to each other in alternate rows of molecules. [CO ligands and H atoms are not shown for clarity. Shaded spheres represent the C(benzene) atoms]

The overall intermolecular assembly in the two polymorphic forms **2** and **2a** is very similar. The space-filling projections given in Figs. 4(*a*) and 4(*b*) for species **2** and **2a**, respectively, allow one to see that while the benzene ligands are parallel to each other in crystalline **2**, in crystalline **2a** there are alternate rows of molecules in which the benzene units are *ca.* 90° to each other. As in the case of **2** the benzene ligands are almost perpendicular to the *bc* plane. Apart from the different relative orientations of the molecules the molecular distribution is very similar thus accounting for the close similarity of the two crystalline cells.

Conclusion

The comparative analysis of the crystal and molecular structures of **1**–**3** has allowed insight into the factors controlling the structural choice of flexible organometallic molecules in the solid state. The disorder observed in crystalline **2** has been shown to originate from a dynamic process which does not take place in the denser crystal structure of the second

Table 5 Crystal data and details of measurements for **1**–**3**

Complex	**1**	**2**	**3**
Formula	$C_{18}H_8O_{12}Ru_4$	$C_{21}H_{14}O_9Ru_4$	$C_{21}H_{14}O_9Ru_4$
M	820.5	814.5	814.5
T/K	150	296	150
Crystal system	Monoclinic	Monoclinic	Monoclinic
Space group	$P2_1/c$	Cc	$P2_1/c$
a/Å	9.779(8)	10.010(3)	16.655(3)
b/Å	22.163(14)	15.532(4)	15.709(3)
c/Å	10.069(6)	15.384(4)	17.831(4)
β/°	90.23(9)	93.50(2)	91.44(3)
U/Å^3	2182(3)	2378(1)	4664(2)
Z	4	4	8
F(000)	1552	1552	3104
D_c/g cm^{-3}	2.50	2.29	2.32
λ(Mo-Kα)/Å	0.710 73	0.710 69	0.710 73
μ(Mo-Kα)/cm^{-1}	2.779	2.329	2.591
θ range/°	2.5–25	3.5–30.0	2.5–22.5
Octants explored *hkl*	−11 to 11, 0–26, 0–11	−14 to 14, 0–21, 0–21	0–17, 0–17, −19 to 19
Unique observed reflections	3819	3571	6043
Unique observed reflections with [$I_o > 2\sigma(I_o)$]	3408	3464	4973
No. of refined parameters	308	327	403
GOF on F^2	1.205	1.214	1.207
$R1$ [on F, $I > 2\sigma(I)$]	0.0238	0.0277	0.0706
$wR2$ (on F^2, all data)	0.0658	0.0748	0.2563

Table 6 Atomic coordinates (× 10^4) for **1**

Atom	x	y	z
Ru(1)	729(1)	8 592(1)	2 804(1)
Ru(2)	2 458(1)	9 554(1)	3 162(1)
Ru(3)	3 395(1)	8 445(1)	3 910(1)
Ru(4)	2 692(1)	7 937(1)	1 543(1)
C(1)	−29(5)	8 754(2)	4 522(5)
O(1)	−512(4)	8 830(2)	5 535(3)
C(2)	−725(5)	8 978(2)	1 842(5)
O(2)	−1 592(4)	9 210(2)	1 301(4)
C(3)	−116(5)	7 820(2)	2 724(5)
O(3)	−718(4)	7 378(2)	2 710(4)
C(4)	4 074(5)	10 033(2)	3 391(4)
O(4)	5 044(4)	10 304(2)	3 532(3)
C(5)	1 443(5)	10 187(2)	2 290(5)
O(5)	826(5)	10 547(2)	1 773(4)
C(6)	1 828(5)	9 800(2)	4 854(5)
O(6)	1 475(4)	9 956(2)	5 870(3)
C(7)	5 295(5)	8 602(2)	4 186(5)
O(7)	6 420(4)	8 714(2)	4 309(4)
C(8)	2 846(5)	8 641(2)	5 690(5)
O(8)	2 539(4)	8 728(2)	6 772(3)
C(9)	3 442(5)	7 608(2)	4 386(5)
O(9)	3 491(4)	7 121(2)	4 760(4)
C(10)	2 197(5)	7 135(2)	2 049(5)
O(10)	1 925(4)	6 655(2)	2 329(4)
C(11)	1 943(5)	7 798(2)	−184(5)
O(11)	1 489(4)	7 728(2)	−1 217(3)
C(12)	4 475(5)	7 665(2)	1 111(5)
O(12)	5 564(4)	7 525(2)	891(4)
C(13)	3 560(5)	8 848(2)	1 980(4)
C(14)	2 192(5)	8 925(2)	1 434(4)
C(15)	1 957(5)	9 215(2)	70(4)
C(16)	3 247(5)	9 513(2)	−467(5)
C(17)	4 470(5)	9 109(2)	−283(4)
C(18)	4 825(5)	9 031(2)	1 202(4)

Table 7 Atomic coordinates (× 10^4) for **2**

Atom	x	y	z
Ru(1)	7 651(1)	2 660(1)	−517(1)
Ru(2)	7 509(1)	2 369(1)	1 209(1)
Ru(3)	6 740(1)	1 095(1)	149(1)
Ru(4)	8 899(1)	1 152(1)	−773(1)
C(1)	5 937(7)	2 603(4)	−1 130(4)
O(1)	4 936(6)	2 554(4)	−1 488(4)
C(2)	7 450(7)	3 796(4)	−79(5)
O(2)	7 349(7)	4 506(3)	106(5)
C(3)	8 620(7)	3 032(6)	−1 459(5)
O(3)	9 212(8)	3 284(7)	−2 024(5)
C(4)	7 373(6)	1 790(5)	2 293(4)
O(4)	7 255(7)	1 402(6)	2 903(4)
C(5)	8 343(7)	3 353(5)	1 783(4)
O(5)	8 802(7)	3 950(4)	2 085(4)
C(6)	5 740(7)	2 800(4)	1 190(4)
O(6)	4 699(6)	3 068(5)	1 165(5)
C(7)	10 582(8)	1 383(6)	−1 238(5)
O(7)	11 591(8)	1 535(8)	−1 513(6)
C(8)	9 236(8)	−37(5)	−677(7)
O(8)	9 343(9)	−777(4)	−609(8)
C(9)	7 853(9)	1 110(6)	−1 815(6)
O(9)	7 239(9)	1 075(6)	−2 461(5)
C(13)	8 675(5)	1 299(3)	667(4)
C(14)	9 197(5)	2 093(3)	354(3)
C(15)	10 606(6)	2 398(4)	627(4)
C(18)	9 528(7)	715(5)	1 290(5)
C(16)	11 446(14)	1 652(9)	990(9)
C(17)	10 722(18)	1 189(11)	1 704(11)
C(16D)	11 272(18)	1 917(13)	1 369(14)
C(17D)	10 977(19)	993(12)	1 337(23)
C(19)	5 044(8)	588(6)	−681(5)
C(20)	4 503(6)	1 048(5)	−6(5)
C(21)	4 869(7)	831(5)	855(5)
C(22)	5 799(8)	204(5)	1 049(6)
C(23)	6 322(9)	−259(5)	404(9)
C(24)	5 905(9)	−80(6)	−509(8)

polymorph **2a**. Weak C–H ••• O hydrogen-bonding interactions have been shown to participate in the pattern of intermolecular interactions.

We have previously established a detailed and systematic chemistry of cyclohexadiene and arene derivatives based on the Os_4 tetrahedral cluster unit.[18] In that there was little evidence for the activation of olefinic C–H bonds to generate 'yne'-derivatives. In contrast, we now find that for ruthenium the tetrahedral unit is not observed, and in its place the chemistry is dominated by the formation of the *closo*-Ru_4C_2 octahedral core. The Ru_4 butterfly arrangement within this core closely resembles the step-site of a metal surface and it is tempting to associate or relate the chemistry with that observed for these sites. Certainly the butterfly clusters reported here form a reasonable geometric analogue of the surface step.

Table 8 Atomic coordinates (× 10^4) for **3**

Atom	*x*	*y*	*z*	Atom	*x*	*y*	*z*
Ru(1)	4 729(1)	1 662(1)	6 118(1)	Ru(5)	10 712	2 389	7 712
Ru(2)	4 991(1)	3 285(1)	6 620(1)	Ru(6)	9 987	3 454	8 699
Ru(3)	5 806(1)	1 999(1)	7 322(1)	Ru(7)	9 671(1)	1 754(1)	8 796(1)
Ru(4)	6 341(1)	1 407(1)	6 000(1)	Ru(8)	11 282(1)	1 399(1)	8 849(1)
C(1)	4 869(12)	490(14)	6 173(12)	C(31)	9 707(12)	548(14)	8 736(12)
O(1)	4 886(9)	−283(10)	6 223(9)	O(31)	9 637(9)	−169(11)	8 743(9)
C(2)	4 160(12)	1 801(13)	5 149(12)	C(32)	8 983(12)	1 829(13)	9 655(12)
O(2)	3 846(10)	1 906(11)	4 626(9)	O(32)	8 583(9)	1 907(10)	10 127(9)
C(3)	3 755(12)	1 642(13)	6 651(12)	C(33)	8 803(13)	1 791(14)	8071(13)
O(3)	3 151(9)	1 594(11)	6 968(9)	O(33)	8 283(9)	1 784(10)	7 643(9)
C(4)	4 344(14)	3 938(16)	5 902(14)	C(34)	9 545(12)	3 955(13)	9 572(12)
O(4)	3 966(12)	4 311(12)	5 480(11)	O(34)	9 326(10)	4 272(11)	10 093(10)
C(5)	4 144(15)	3 320(15)	7 345(14)	C(35)	8 982(13)	3 647(14)	8 158(12)
O(5)	3 675(10)	3 353(10)	7 765(10)	O(35)	8 415(8)	3 809(9)	7 861(9)
C(6)	5 504(15)	4 292(17)	7 043(14)	C(36)	10 506(14)	4 476(15)	8 343(13)
O(6)	5 839(11)	4 859(10)	7 251(10)	O(36)	10 806(9)	5 038(11)	8 099(10)
C(7)	4 960(14)	1 830(15)	8 016(13)	C(37)	9 885(13)	2 757(14)	7 009(13)
O(7)	4 452(9)	1 726(10)	8 433(10)	O(37)	9 414(11)	2 983(14)	6 608(9)
C(8)	6 517(13)	2 629(14)	7 990(13)	C(38)	11 517(14)	2 997(15)	7 211(13)
O(8)	6 922(9)	2 976(11)	8 388(8)	O(38)	11 969(10)	3 400(10)	6 893(10)
C(9)	6 230(15)	917(17)	7 592(15)	C(39)	10 887(12)	1 319(14)	7 261(12)
O(9)	6 453(10)	243(10)	7 816(9)	O(39)	10 912(10)	699(9)	6 912(9)
C(13)	6 162(10)	2 715(11)	6 361(10)	C(43)	10 644(11)	2 417(12)	9 372(11)
C(14)	5 612(12)	2 511(13)	5 741(12)	C(44)	11 179(11)	2 792(12)	8 806(10)
C(15)	5 678(12)	2 931(14)	4 946(12)	C(45)	11 908(11)	3 330(13)	9 016(11)
C(16)	6 479(13)	3 482(15)	4 856(13)	C(46)	11 811(13)	3 699(13)	9 802(12)
C(17)	6 703(13)	3 953(14)	5 603(12)	C(47)	11 607(13)	3 017(14)	10 362(13)
C(18)	6 877(12)	3 353(13)	6 241(12)	C(48)	10 777(11)	2 573(13)	10 215(11)
C(19)	7 316(12)	1 419(13)	5 185(12)	C(49)	12 438(13)	1 239(14)	9 449(13)
C(20)	7 663(13)	1 273(14)	5 882(13)	C(50)	12 549(12)	1 101(14)	8 681(12)
C(21)	7 389(12)	590(13)	6 318(12)	C(51)	12 110(13)	478(14)	8 324(14)
C(22)	6 747(13)	83(14)	6 048(13)	C(52)	11 521(12)	39(13)	8 703(12)
C(23)	6 416(12)	239(13)	5 337(11)	C(53)	11 394(13)	199(14)	9 458(12)
C(24)	6 700(12)	880(14)	4 894(13)	C(54)	11 852(13)	792(14)	9 834(13)

The unusual reversible isomerization observed in this work appears to form part of an emerging pattern which seems to suggest that, contrary to expectation, polytopal rearrangement of cluster atom geometries may be a regular feature of these compounds at higher temperatures, and we are attempting to design experiments to test this hypothesis.

Experimental

All reactions were carried out with the exclusion of air using solvents freshly distilled under an atmosphere of dry nitrogen. Subsequent work-up of products was achieved without precautions to exclude air with standard laboratory grade solvents. Infrared spectra were recorded on a Perkin-Elmer 1600 Series FTIR in CH_2Cl_2 using NaCl cells. Positive fast atom bombardment mass spectra were obtained using a Kratos MS50TC spectrometer, with CsI as calibrant. Proton NMR spectra were recorded in $CDCl_3$ using a Bruker AM250 instrument, referenced to internal $SiMe_4$. Products were separated by thin layer chromatography on plates supplied by Merck coated with a 0.25 mm layer of Kieselgel 60 F_{254}, using dichloromethane–hexane (30:70) eluent. Cyclohexa-1,3-diene and trimethylamine *N*-oxide (Me_3NO) were purchased from Aldrich Chemicals. Trimethylamine *N*-oxide was purchased as the dihydrate and sublimed immediately prior to reaction.

Thermolysis of $[Ru_3(CO)_{12}]$ *with Cyclohexa*-1,3-*diene in Octane*.—The compound $[Ru_3(CO)_{12}]$ (250 mg) in octane (30 cm^3) containing cyclohexa-1,3-diene (5 drops) was heated to reflux for 1 h, during which time the solution darkened quite substantially. Excess of cyclohexa-1,3-diene (2 cm^3) was added, and the reaction was monitored by spot TLC which indicated complete consumption of starting material after this time. The solvent was removed *in vacuo* and the products separated by TLC. Four main bands, in order of elution, were isolated and characterized by spectroscopy as $[Ru_4(CO)_{12}(\mu_4\text{-}\eta^2:\eta^2\text{-}C_6H_8)]$ **1** (red, 22%), $[Ru_4(CO)_9(\mu_4\text{-}\eta^2:\eta^2\text{-}C_6H_8)(\eta^6\text{-}C_6H_6)]$ **2** (purple, 6%) and the known compound $[Ru_6(CO)_{14}(\eta^6\text{-}C_6H_6)]$ **4** (brown, 16%).

Thermolysis of $[Ru_4(CO)_{12}(\mu_4\text{-}\eta^2:\eta^2\text{-}C_6H_8)]$ **1** *with Cyclohexa*-1,3-*diene in Octane*.—Cyclohexa-1,3-diene (1 cm^3) was added to a solution of compound **1** (50 mg) in octane (25 cm^3) and heated to reflux for 3 h. The solvent was removed under reduced pressure and the residue purified by TLC. Several bands were obtained in low yield, of which the major product was characterized as **2** (18%).

Reaction of $[Ru_4(CO)_{12}(\mu_4\text{-}\eta^2:\eta^2\text{-}C_6H_8)]$ **1** *with Cyclohexa*-1,3-*diene and* Me_3NO.—The compound $[Ru_4(CO)_{12}(\mu_4\text{-}\eta^2:\eta^2\text{-}C_6H_8)]$ **1** (50 mg) was dissolved in dichloromethane (50 cm^3), an excess of cyclohexa-1,3-diene (1–2 cm^3) was added and the solution cooled to −78 °C. A solution of Me_3NO (15 mg, 3.2 mol equivalent) in dichloromethane (20 cm^3) was added dropwise over 10 min and the reaction mixture allowed to warm to room temperature where it was stirred for a further hour. The solvent was removed *in vacuo* and the products separated by TLC. Two main products were extracted which, in order of elution, were characterized spectroscopically as **2** (4%) and **3** (18%).

The Interconversion of Isomers **2** *and* **3**.—A solution of $[Ru_4(CO)_9(\mu_4\text{-}\eta^2:\eta^2\text{-}C_6H_8)(\eta^6\text{-}C_6H_6)]$ **3** (10 mg) in octane (30 cm^3) was heated under reflux for 2 h. During this time the solution changed from purple to red, and IR spectroscopy indicated complete consumption of the starting material to give $[Ru_4(CO)_9(\mu_4\text{-}\eta^2:\eta^2\text{-}C_6H_8)(\eta^6\text{-}C_6H_6)]$ **2** (90%). This was confirmed by spot TLC which showed no other products present, and that virtually no decomposition had taken place during the reaction. However on standing at room temperature, a dichloromethane solution of **2** reverted slowly back to **3**, as evidenced by IR spectroscopy and spot TLC.

Structural Characterization.—Crystallographic data and details of measurements for the structures are given in Table 5. All data were corrected for Lorentz and polarization effects. Absorption corrections were applied in the cases of structures **2** and **3** by azimuthal scanning of high-χ (> 80°) reflections (min. and max. transmission 0.81, 1.00 and 0.91, 1.00, respectively), and by the Walker and Stuart method [19a] in the case of **1** (min. and max. corrections 0.92, 1.12). The three structures were solved by direct methods and the refinement was carried out by least-squares full-matrix cycles using the SHELXL 93 system of computer programs [19b] with, initially, isotropic and then anisotropic thermal parameters on the Ru and O atoms in all cases, and also on the C atoms in structures **1** and **2**. Attempts to locate the hydrogen atoms from the Fourier map were successful for structure **1**, but failed for structures **2** and **3**, and the positions were calculated. In all cases the hydrogens were allowed to refine riding on the corresponding C atoms. The disorder corresponding to the two different orientations of the C_6H_8 ligand was observed from the Fourier map of **2**. Site-occupation factors for the other CH_2CH_2 unit refined to values close to 0.5 for both orientations. This value was adopted to subsequently refine the anisotropic thermal parameters. Fractional atomic coordinates are reported in Tables 6, 7 and 8 for **1**, **2** and **3**, respectively.

Additional material available from the Cambridge Crystallographic Data Centre comprises H-atom coordinates, thermal parameters and remaining bond lengths and angles.

Acknowledgements

The Ministero dell'Università e della Ricerca Scientifica e Tecnologica (D. B., F. G.) is acknowledged. D. B., F. G. and B. F. G. J. thank NATO for a travel grant. The ERASMUS 'Crystallography' scheme for student exchange between Universities is acknowledged (J. B.). C. M. M. and B. F. G. J. thank the EPSRS, ICI (Wilton) and the University of Edinburgh for financial support.

References

1 D. Braga, P. J. Dyson, F. Grepioni and B. F. G. Johnson, *Chem. Rev.*, 1994, **94**, 1585.
2 P. J. Dyson, B. F. G. Johnson, J. Lewis, M. Martinelli, D. Braga and F. Grepioni, *J. Am. Chem. Soc.*, 1993, **115**, 9602.
3 D. Braga, P. J. Dyson, F. Grepioni, B. F. G. Johnson and M. J. Calhorda, *Inorg. Chem.*, 1994, **33**, 3218.
4 D. Braga and F. Grepioni, *Acc. Chem. Res.*, 1994, **27**, 51.
5 D. Braga and F. Grepioni, *J. Chem. Soc., Dalton Trans.*, 1993, 1223; D. Braga, F. Grepioni, E. Parisini, B. F. G. Johnson, M. C. Martin, J. G. M. Nairn, J. Lewis and M. Martinelli, *J. Chem. Soc., Dalton Trans.*, 1993, 1891.
6 D. Braga, F. Grepioni, P. Sabatino and G. R. Desiraju, *Organometallics*, 1994, **13**, 3253; D. Braga, F. Grepioni, K. Biradha, V. R. Pedireddi and G. R. Desiraju, *J. Am. Chem. Soc.*, in the press.
7 S. Aime, L. Milone, D. Osella, M. Vaglio, A. Tiripicchio and M. Tiripicchio-Camellini, *Inorg. Chim. Acta*, 1979, **34**, 49.
8 B. F. G. Johnson, J. Lewis, B. Reichert, K. T. Schorpp and G. M. Sheldrick, *J. Chem. Soc., Dalton Trans.*, 1977, 1417; B. F. G. Johnson, J. Lewis and K. T. Schorpp, *J. Organomet. Chem.*, 1975, **91**, C13.
9 P. F. Jackson, B. F. G. Johnson, J. Lewis, P. R. Raithby, G. J. Will, M. McPartlin and W. J. H. Nelson, *J. Chem. Soc., Chem. Commun.*, 1980, 1190.
10 D. Braga, F. Grepioni, P. Sabatino, P. J. Dyson, B. F. G. Johnson, J. Lewis, P. Raithby and D. Stalke, *J. Chem. Soc., Dalton Trans.*, 1993, 985.
11 D. Braga, *Chem. Rev.*, 1992, **92**, 633.
12 D. Braga, F. Grepioni and E. Parisini, *Organometallics*, 1991, **10**, 3735.
13 A. I. Kitaigorodski, *Molecular Crystal and Molecules*, Academic, New York, 1973.
14 D. Braga and F. Grepioni, *Organometallics*, 1991, **10**, 2563; *Organometallics*, 1992, **11**, 711; D. Braga, F. Grepioni and P. Sabatino, *J. Chem. Soc., Dalton Trans.*, 1990, 3137.
15 A. Gavezzotti, OPEC, University of Milano, 1983; see also A. Gavezzotti, *J. Am. Chem. Soc.*, 1983, **195**, 5220.
16 A. L. Spek, PLATON, *Acta Crystallogr., Sect. A*, 1990, **46**, C31.
17 E. Keller, SCHAKAL92, *Graphical Representation of Molecular Models*, University of Freiburg, Freiburg, 1992.
18 B. F. G. Johnson, A. J. Blake, C. M. Martin, D. Braga, E. Parisini and H. Chen, *J. Chem. Soc., Dalton Trans.*, 1994, 2167.
19 (*a*) N. Walker and D. Stuart, *Acta Crystallogr., Sect. B*, 1983, **39**, 158; (*b*) G. M. Sheldrick, SHELXL 93, *Program for Crystal Structure Determination*, University of Göttingen, Göttingen, 1992.

Received 21*st October* 1994; *Paper* 4/06467D